Sequential binding and sensing of Zn(II) by *Bacillus subtilis* Zur

Zhen Ma, Scott E. Gabriel and John D. Helmann*

Department of Microbiology, Cornell University, Ithaca, NY 14853-8101, USA

ABSTRACT

Bacillus subtilis **Zur (BsZur) represses high-affinity zinc-uptake systems and alternative ribosomal proteins in response to zinc replete conditions. Sequence alignments and structural studies of related Fur family proteins suggest that BsZur may contain three zinc-binding sites (sites 1–3). Mutational analyses confirm the essential structural role of site 1, while mutants affected in sites 2 and 3 retain partial repressor function. Purified BsZur binds a maximum of two Zn(II) per monomer at site 1 and site 2. Site 3 residues are important for dimerization, but do not directly bind Zn(II). Analyses of metal-binding affinities reveals negative cooperativity between the two site 2 binding events in each dimer. DNA-binding studies indicate that BsZur is sequentially activated from an inactive dimer ($Zur_2{:}Zn_2$) to a partially active asymmetric dimer ($Zur_2{:}Zn_3$), and finally to the fully zinc-loaded active form ($Zur_2{:}Zn_4$). BsZur with a C84S mutation in site 2 forms a $Zur_2{:}Zn_3$ form with normal metal- and DNA-binding affinities but is impaired in formation of the $Zur_2{:}Zn_4$ high affinity DNA-binding state. This mutant retains partial repressor activity *in vivo*, thereby supporting a model in which stepwise activation by zinc serves to broaden the physiological response to a wider range of metal concentrations.**

INTRODUCTION

Fur family proteins define one of seven major groups of metalloregulators in bacteria (1,2). Fur was first described in *Escherichia coli* as playing a central role in iron homeostasis (3). Fur and Fur-like proteins have now been identified in many bacterial species and, in addition to iron, sense a variety of other metal ions. Examples include sensing of Zn(II) by Zur, Mn(II) by Mur, Ni(II) by Nur and hydrogen peroxide by PerR (1). Typically,

Fur family proteins function with a metal ion co-repressor to down-regulate genes involved in metal uptake. Fur-dependent positive regulation has also been observed and is often mediated indirectly via antisense small RNAs (1,2,4).

The detailed molecular basis for metal-sensing by Fur family proteins has been a puzzle, despite the availability of several high resolution crystal structures. Sequence alignments and structural studies suggest that Fur family proteins may contain as many as three metal-binding sites. *Bacillus subtilis* encodes three Fur orthologs named Fur, Zur and PerR, involved in iron, zinc and iron-dependent peroxide sensing, respectively (4–8). These three paralogs each contain three candidate metal-binding sites which we designate as site 1 (a Cys_4 structural zinc site), site 2 (E70, C84, H90 and H92) and site 3 (H89, H91, D110 and H124) where the numbering corresponds to the predicted ligands in BsZur (Figure 1A). The Cys_4-Zn(II) structural site (site 1) is close to the C-terminus and is known to be important for the stability and function of both PerR and Fur (9,10). The identity of the sensing site has only been well characterized in PerR, in which a penta-coordinated square pyramidal geometry was observed at site 2 (11,12). Residues corresponding to site 3 were apparently not involved directly in metal-coordination but were proposed instead to form a hydrogen-bonding network that affects metal selectivity for site 2 binding (13).

Although two to three Zn(II) atoms have been visualized in several Fur family structures [including *Pseudomonas aeruginosa* Fur (PaFur), *Mycobacterium tuberculosis* Zur (MtZur), *Vibrio cholerae* Fur (VcFur), *Helicobacter pylori* Fur (HpFur) and *Streptomyces coelicolor* Zur (ScZur) (14–18)] the metal-binding stoichiometries and affinities, and the effects each metal-binding event has on DNA-binding affinity, are generally unclear. Moreover, those biochemical studies that have been done are often for proteins where no crystal structure is available or where one or more of these sites is lacking (19–22). Thus, the site(s) required for metal-sensing *in vivo* have not been unambiguously defined. Since site 2 is required for iron-dependent

protein oxidation of PerR (8,11), a parsimonious model is that site 2 is generally involved in metal sensing. Evidence in support of this model has been provided for HpFur, but in this case mutations in site 3 also had modest effects on metal responsiveness (14). Genetic analyses are complicated by the fact that sites 2 and 3 are physically close to each other and ligands are contributed from a shared loop region which may allow ligand reassignment in mutant proteins.

We show here that in BsZur only site 2 is involved directly in Zn(II)-sensing whereas site 3 residues appear to be crucial for dimerization. Measurements of metal- and DNA binding affinities support a model in which a Zur dimer, containing two structural Zn(II) atoms, binds two additional Zn(II) ions with negative cooperativity at site 2. This results in a sequential activation first to an asymmetric dimer (Zur_2:Zn_3) with moderate DNA binding activity and finally to the fully zinc-loaded, high affinity DNA-binding species (Zur_2:Zn_4). These biochemical analyses provide new insights into the variety of molecular mechanisms used by Fur family metalloregulators for metal binding and sensing.

MATERIALS AND METHODS

Bacillus subtilis strain constructions and β-galactosidase assays

BsZur variants with a C-terminal FLAG-tag were integrated at the *amyE* locus of strain HB9700 (CU1065 *zur::tet*) (23). Promoter-*lacZ* fusions were constructed using the HindIII and BamHI restriction sites of the pJPM122 integrational plasmid (24). The resulting plasmids were transformed into the SPβ prophage carried in strain ZB307A as described (24). Heat induction was used to obtain SPβ lysates to transduce the reporter fusion into *B. subtilis* strains as described (23). For β-galactosidase assays, 5 ml LB was inoculated with 50 μl overnight culture and grown to mid-logarithmic phase ($OD_{600} \approx 0.4$) at 37°C. Cells were harvested by centrifugation and the β-galactosidase assay was carried out as described (25), except that cells were lysed by addition of lysozyme to a final concentration of 20 μg/mL followed by a 30-min incubation at 37°C. All assays were performed in triplicate and the values were averaged.

Purification of BsZur

The coding sequence for WT BsZur was cloned into pET16b (Novagen) between the NcoI and BamHI restriction sites. For BsZur mutants, plasmids were constructed using quick change site-directed mutagenesis and transformed into *E. coli* strain BL21(DE3/pLysS) with selection for Cm^R and Amp^R. A single colony was grown in LB at 37°C and an overnight culture was inoculated (1:100) into 1 L fresh LB containing 0.5% (w/v) glucose. Cells were grown at 37°C until OD_{600} ∼0.5, after which cells were induced with 1 mM IPTG in the presence of 50 μM $ZnSO_4$ (final concentrations) and grown at 30°C for 4 h. Cells harvested by low speed centrifugation were resuspended in 10 mL buffer A [20 mM Tris, pH 8.0, 100 mM

NaCl, 2 mM EDTA, 2 mM DTT, 5% glycerol (v/v)] and lysed by sonication. The resulting supernatant containing BsZur was subjected to a three-step purification protocol with haperin column, Superdex 200 size exclusion column and MonoQ column as described (26). Purified BsZur was dialyzed against buffer B [20 mM Tris, pH 8.0, 0.1 M NaCl, 1 mM TCEP (tris(2-carboxyethyl)-phosphine)] and were >90% pure as visualized by SDS–PAGE. The protein concentration was determined by A_{277} using a calculated extinction coefficient of 13 785 $M^{-1} cm^{-1}$ and are expressed as protein monomer. Zinc content of the purified proteins, which usually varies between 0.5–0.8 Zn(II) per monomer (Table 1), was determined by a PAR (4-(2-pyridylazo)-resorcinol) assay as described (9).

Zn(II) binding monitored by FluoreZin-3 (Fz3) and Quin-2 competition

All Zn(II) binding experiments were carried out in buffer B containing 0.1 mM TCEP. TCEP prevents Cys oxidation and 0.1 mM TCEP showed no interference with Zn(II) binding in the presence of the competitors used here (data not shown). For competition with Fz3, BsZur (150–400 nM) was mixed with 195 nM Fz3 in a quartz cuvette (final volume 3 mL). After each addition of Zn(II), samples were equilibrated for 5 min before the emission spectra (505–600 nm) were collected (excitation wavelength 494 nm). Maximal emission (517 nm) was plotted against [Zn(II)]. For competition with Quin-2, 10–20 μM BsZur monomer was mixed with 10.7 μM Quin-2 in a quartz cuvette (final volume 900 μL). After each addition of Zn(II), UV-vis spectra were collected after 10 min of equilibration and A_{261} plotted against [Zn(II)]. All data were fit to a competition model involving two independent Zn(II) binding events using Dynafit (27).

Co(II) titration

Co(II) titrations were carried out in buffer B containing 0.1 mM TCEP. Increasing amounts of Co(II) were added to 900 μL of BsZur (20–40 μM). UV-vis spectra from 210–800 nm were recorded after each addition. After saturation, a back titration with Zn(II) was carried out. Five minutes of equilibration time was allowed before the

Table 1. Zn(II) binding stoichiometry[a] and affinities of WT and BsZur mutants

BsZur	Zn(II) content[b]	n_1[c]	K_{Zn1} ($\times 10^{12} M^{-1}$)	n_2[c]	K_{Zn2} ($\times 10^9 M^{-1}$)
WT	0.53	0.9 (0.97)	18 (±6)	0.5	830 (±100)
C84S	0.80	0.7 (0.70)	18 (±6)	0.5	0.047 (±0.004)[d]
H90A	0.72	0.8 (0.78)	2.7 (±0.4)	0.5	0.033 (±0.007)[d]
H89A	0.62	0.9 (0.88)	6.7 (±0.4)	0.5	12 (±2)
H124A	0.65	0.9 (0.85)	3.6 (±0.2)	0.5	3600 (±200)

[a]All numbers based on molar equivalent of BsZur monomer.
[b]Zn(II) content in purified BsZur as determined by PAR assay.
[c]Stoichiometry used in data fitting corresponding to the two independent Zn(II) binding to BsZur dimer with expected stoichiometry in parenthesis. Expected n_2 are 0.50 in all cases.
[d]Determined by competition with Fz3; all other Zn(II) affinities were determined with Quin-2.

UV-vis spectra were taken. This time period ensures the full exchange at the 'sensing' site but not at the structural site.

Superdex G75 size exclusion chromatography

A superdex G75 10/300 GL column was equilibrated with buffer C (20 mM Tris, pH 8.0, 0.2 M NaCl, 1 mM TCEP). A total of 200 μL of 2 μM BsZur was loaded onto the column and 0.5 mL fractions were collected. A total of 160 μl from each fraction was then mixed with 40 μL of Bio-Rad protein assay dye reagent on a microtiter plate as described by the microassay protocol in the product instructions. After 10 min of incubation, the absorbance at 595 nm was measured using a plate reader. The absorbance represents the relative amount of protein in each faction and was directly plotted against the corresponding elution volume.

DNA binding by fluorescence anisotropy

A 6-carboxyfluorescein (6-FAM) labeled double-strand DNA containing the *zur*-box (bold) derived from the *yciA* promoter (5′-6-FAM-GGA**AATAGTAATTATTAC GATT**TGG-3′ and the unlabeled complement) was used. BsZur was titrated into 2 mL of 10 nM DNA probe in buffer C with 1 mM EDTA, 100 μM nitrilotriacetic acid (NTA) or 1 μM Zn(II). For C84S and H90A BsZurs with low Zn(II) binding affinities, 100 μM Zn(II) was used to ensure all the proteins were Zn(II)-saturated. Fluorescence anisotropy (λ_{ex} = 495 nm; λ_{em} = 520 nm) was measured after each addition of BsZur and 2 min equilibration. The average of six continuous measurements for each addition are reported. The magnitude of change in anisotropy was similar in all experiments. Binding affinities were obtained by fitting the data using a non-dissociable dimer binding to DNA (1:1) model by Dynafit (27). For Zn(II) activation experiments, Zn(II) was titrated into a mixture of 10 nM DNA in buffer C with 200 μM EDTA and 0.10 or 1.0 μM BsZur. Equilibration time of 10 min was allowed before each measurement. The resulting data were fit by Dynafit with a multiple equilibria model including both Zn(II) and DNA binding (27).

RESULTS

Repressor activities of BsZur variants *in vivo*

Alignment of BsZur with structurally and functionally characterized Fur family proteins revealed potential conservation of residues in all three metal-binding sites (Figure 1A and Supplementary Figure S1). We introduced substitution mutations of putative metal ligands to test the role of each predicted metal-binding site on repressor activity, which was measured by monitoring repression of the *yciC* promoter under zinc replete conditions (6,26). As expected, the *yciC* promoter was fully repressed in strains carrying wild-type (WT) BsZur or BsZur-FLAG when grown in LB but derepressed in a *zur*-null strain (Figure 1B). Since the BsZur-FLAG protein appeared fully functional, and the epitope tag provides a convenient means for monitoring protein accumulation and stability

in vivo, this survey was conducted using epitope-tagged Zur proteins.

Mutations in site 1 (C95S, C98S, C132S and C135S) led to either a partial or a full loss of repressor activity (Figure 1B). Western blot analysis revealed that these mutants were severely impaired in their ability to form a stable SDS-resistant Cys₄-Zn(II) structure as observed for WT BsZur-FLAG (Supplementary Figure S2) (9), consistent with a structural role of site 1. These results are reminiscent of prior studies of the corresponding residues in PerR (9) and Fur (10).

No single mutation in putative metal ligands in site 2 or site 3 abolished repressor activity. Moreover, even many double and triple mutants were at least partially active as repressors (Figure 1B). Partial repressor activity was also observed when representative mutants were tested against five other *zur*-regulated promoter–*lacZ* fusions (Supplementary Figure S3 and data not shown). All these mutants accumulated to near normal levels in the cell suggesting that the reduced efficacy in repressor function was not caused by reduced protein levels (data not shown). We conclude that site 2 and site 3 affect BsZur function, but whether or not these mutations affect Zn(II) binding was unclear. Moreover, since BsZur regulates Zn(II) uptake, any repressor with reduced Zn(II) affinity is predicted to allow cellular Zn(II) concentrations to rise to the level needed to compensate for this reduced affinity. To better understand the roles of sites 2 and 3, we therefore developed assays to monitor metal binding directly.

WT BsZur binds only two Zn(II) per dimer in addition to the structural Zn(II) site

For biochemical analysis, BsZur was purified after overproduction in *E. coli*. To remove any adventitiously associated metal ions, purification was conducted in buffers containing 2 mM EDTA and under these conditions there was some loss of the tightly associated structural zinc (corresponding to site 1, see below) with the resulting protein containing 0.5–0.8 Zn(II) per monomer (Table 1). The Zn(II) binding stoichiometry of purified BsZur was first determined using a low affinity Zn(II) competitor FluoreZin-3 (Fz3: $K_{Zn} = 6.7 \times 10^7 \, M^{-1}$) which becomes fluorescent upon binding Zn(II) (28). When Zn(II) was titrated into a mixture of 150 nM BsZur monomer and 195 nM Fz3, no increase in fluorescence intensity was observed until ~1.5 Zn(II) per BsZur monomer was added, after which Zn(II) formed a complex with Fz3 and saturated at ~1:1 ratio (Figure 2A). This suggests that purified WT BsZur can bind ~1.5 Zn(II) per monomer (3.0 per dimer) with very high affinity ($K_{Zn} \geq 10^9 \, M^{-1}$). Since the WT BsZur used in this experiments contained 0.53 Zn(II) per monomer as purified (determined by PAR assay; Table 1), this is consistent with filling of the structural site and one extra Zn(II) binding site per monomer (a final stoichiometry of 4 Zn(II) per dimer). In this assay, only Zn(II) binding events with an affinity $\geq 10^6 \, M^{-1}$ can be observed. We reasoned that any Zn(II) binding with an affinity $< 10^6 \, M^{-1}$ is unlikely to be physiologically relevant due to the low concentration of bioavailable Zn(II) in the
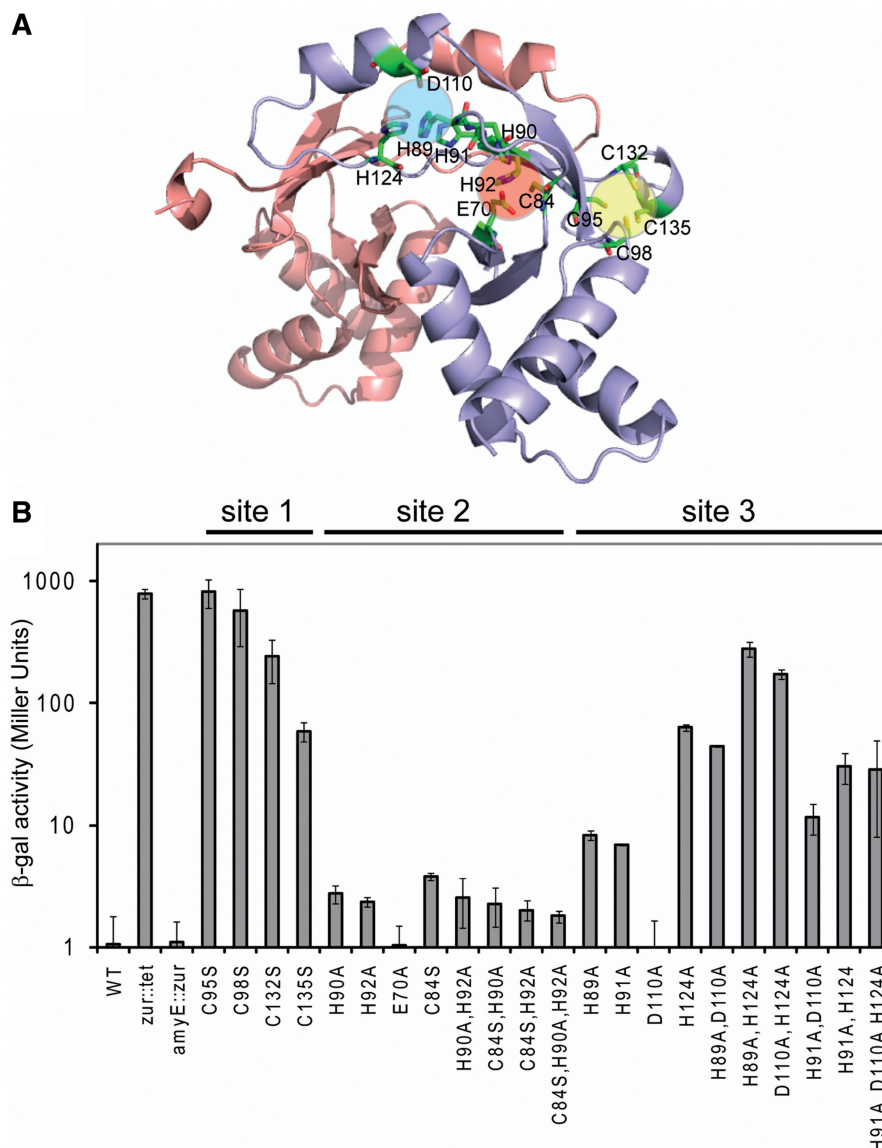
Figure 1. (**A**) Homology model of BsZur dimer using ScZur as template (PDB:3mwm) with putative ligands from site 1 (yellow), site 2 (red) and site 3 (green) highlighted. (**B**) Repressor activities of C-terminal FLAG-tagged WT and BsZur mutants on *yciC* promoter–*lacZ* fusions.

cell (21). We conclude that WT BsZur binds a maximum of 4 Zn(II) ions per dimer with physiologically relevant affinity.

A higher affinity Zn(II) competitor, Quin-2 ($K_{Zn} = 2.7 \times 10^{11}\,M^{-1}$) (29), was used to determine the Zn(II) binding affinity of BsZur. The UV absorbance of Quin-2 is quenched by Zn(II) binding as described (29). When Zn(II) was titrated into a mixture of 11.5 μM BsZur monomer and 10.7 μM Quin-2, competition was observed as indicated by the non-linear decrease in absorbance (Figure 2B). This decrease was saturated at ∼27 μM Zn(II), corresponding to 1.0 mol equiv of Quin-2 plus ∼1.4 mol. equiv. of BsZur monomer, consistent with the stoichiometry determined by the Fz3 competition above. A two independent site binding model best fits the data, giving $K_{Zn1} = 1.8 \ (\pm 0.6) \times 10^{13}\,M^{-1}$ and $K_{Zn2} = 8.3 (\pm 1.2) \times 10^{11}\,M^{-1}$ with the stoichiometry of 0.9 and 0.5

per monomer, respectively (Table 1). These two binding events were tentatively assigned to filling of the unoccupied portion of the structural site (site 1) and the presumed sensing site. Indeed, in multiple binding experiments (Table 1) the high-affinity binding event corresponds to the sum of the unoccupied fraction of the structural site (site 1) and one additional binding event per dimer at the presumed sensing site (site 2, see below). The low-affinity binding event has a stoichiometry of 1 per dimer which we hypothesized represents filling of the second sensing site present in each dimer, as supported by our subsequent studies.

Site 2 is the Zn(II) sensing site

To determine the nature of these two thermodynamically distinct binding events, we monitored metal binding using Co(II) as a surrogate for Zn(II). The characteristic UV-vis
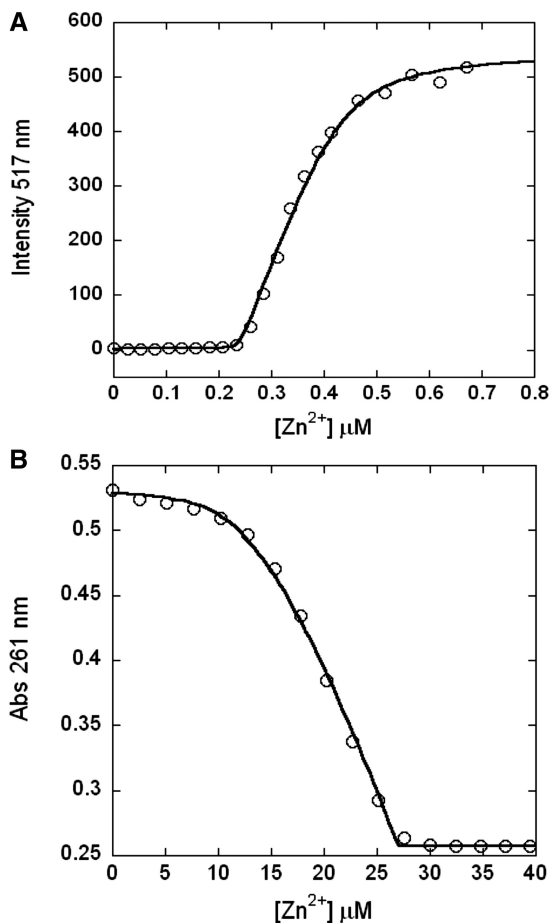
Figure 2. Zn(II) binding stoichiometry and affinity of WT BsZur. (**A**) Fz3 competition. Zn(II) was titrated into 150 nM BsZur monomer and 195 nM Fz3. Lower limits of $10^9 M^{-1}$ were obtained for both K_{Zn1} and K_{Zn2} as indicated by the solid curve. (**B**) Quin-2 competition. Zn(I) was titrated into 10.7 μM Quin-2 and 11.5 μM BsZur monomer. Solid curve represents the best fit with the parameters compiled in Table 1.

Figure 3. Co(II) binding to BsZur. (**A**) Co(II) titration followed by back titration with Zn(II). Zn(II) was added after BsZur was saturated with Co(II) as indicated by the arrow. (**B**) Difference spectra of Co(II) complex in the structural site (solid line) and the sensing site (dashed line) resolved from the titration (see text).

spectral signature of Co(II)-thiolate bonds can be used to distinguish binding at the thiolate-rich structural site 1 (4 Cys thiolates), site 2 (1 thiolate) and site 3 (no thiolate). Site 1 is further distinguished from other sites in that bound metal is predicted to exchange very slowly. Therefore, we used a direct Co(II) titration followed by a Zn(II) back titration to determine the nature of the exchangeable Co(II) that presumably corresponds to binding at the sensing site. We anticipated that the spectrum at the end of the Zn(II) back titration would correspond to a Cys$_4$–Co(II) complex as expected for filling of any vacant structural sites. By subtracting this spectrum from that of the Co(II)-saturated BsZur, the nature of the complex at the sensing site can be resolved.

Co(II) binding to WT BsZur was saturated at ~1.3 Co(II) (1.5 expected) per monomer, consistent with the Zn(II) binding stoichiometry determined above (Figure 3A). Among these, ~0.8 Co(II) per monomer can be readily exchanged with Zn(II), consistent with slow exchange kinetics of the remaining ~0.5 Co(II)
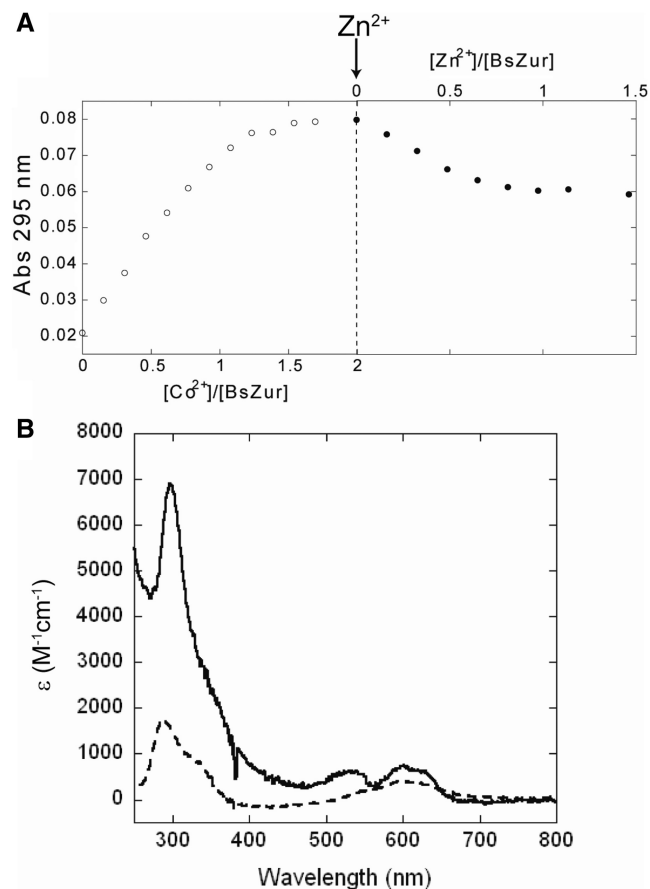
bound at the structural site (Figure 3A). The subtracted spectrum of the Co(II) complex at the structural site (after Zn(II) back titration) exhibits strong ligand to metal charge transfer (LMCT) in the UV region (~297 nm) with an extinction coefficient of ~6900 $M^{-1} cm^{-1}$, as well as strong *d-d* transition at ~600 nm with an extinction coefficient of ~800 $M^{-1} cm^{-1}$ (Figure 3B, solid line). These features are consistent with a S$_4$-coordinated Co(II) in a tetrahedral or distorted tetrahedral geometry as expected (30,31).

Importantly, the resolved difference spectrum for the Co(II)-complex at the sensing site also exhibits LMCT at ~295 nm with an extinction coefficient of ~1750 $M^{-1} cm^{-1}$ and a shoulder at ~340 nm, consistent with at least one Cys in the first coordination shell (Figure 3B, dashed line). A *d–d* transition of ~400 $M^{-1} cm^{-1}$ at ~600 nm suggests a tetrahedral or distorted tetrahedral coordination geometry (30), as commonly observed in many Zn(II) sensing metalloregulatory proteins (2). Therefore, this spectrum shows that the additional ~0.8 Co(II) per monomer is bound at site 2, but not site 3, of WT BsZur. We therefore assigned site 2 as the Zn(II) sensing site.

Site 2 mutants have significantly decreased Zn(II) binding affinities

Zn(II) binding affinities of representative site 2 (C84S and H90A) and site 3 (H89A and H124A) mutants were determined to further support the assignment of site 2 as the Zn(II) sensing site. With Fz3 as competitor, the C84S and H90A mutants bound Zn(II) at a stoichiometry corresponding to saturation of the structural site and an additional 0.5 Zn(II) per monomer (1 per dimer) with high affinity (K_{Zn1}) as indicated by the plateau in the initial part of the binding curve (Supplementary Figure S4A and B). The affinity for the second binding event (K_{Zn2}) was much weaker and best fit with values of $4.7\ (\pm 0.4) \times 10^7\,M^{-1}$ and $3.3\ (\pm 0.7) \times 10^7\,M^{-1}$, respectively (Table 1). Competition with Quin-2 confirmed the K_{Zn1} of $1.8\ (\pm 0.6) \times 10^{13}\,M^{-1}$ for C84S and $2.7\ (\pm 0.4) \times 10^{12}\,M^{-1}$ for H90A, while the binding to the second site (K_{Zn2}) in a dimer was not observed due to the low affinity as expected (Table 1, Supplementary Figure S4C and D).

These data suggest that while the first Zn(II) binding event at site 2 in the BsZur dimer was not strongly affected by mutations in these site 2 ligands (C84S or H90A), the second Zn(II) binding was weakened by ~10^4-fold. In contrast, the site 3 mutants (H89A and H124A) displayed Zn(II) binding affinities comparable to WT BsZur (Table 1, Supplementary Figure S5). The minor decrease in K_{Zn2} in H89A may result from a local conformation change due to the proximity of H89 to the predicted site 2 ligands H90 and H92. Nevertheless, these data strongly support the role of site 2 as the Zn(II) sensing site, while the role of the site 3 residues remains unknown (see below).

The fact that these site 2 mutants (C84S and H90A) were still capable of binding 1 Zn(II) per BsZur dimer with very high affinity was not expected. One interpretation of this result is that site 2 binds Zn(II) with high affinity and that, by analogy with Co(II), this binding normally involves C84 and H90. However, in the absence of C84, ligand recruitment allows the protein to still bind one Zn(II) per dimer with high affinity, but prevents the protein from adopting a conformation suitable for subsequent binding of Zn(II) in the other monomer. Such observations are not unprecedented. For example, the *Staphylococcus aureus* Zn(II)-sensor CzrA also binds two Zn(II) per dimer with negative cooperativity. Some mutations in the first coordination shell affect K_{Zn2} significantly more than K_{Zn1} (31).

Site 3 residues are involved in dimerization

We noticed that the corresponding residue of H124 in MtZur and BsPerR is in a β-strand which is located near the dimer interface (11,16). Therefore, it is possible that H124 may be important for dimer formation. Indeed, $2\,\mu M$ H124A (monomer concentration) appeared to be mainly in the monomer form with or without Zn(II) as shown by size exclusion chromatography (Supplementary Figure S6B). In contrast, WT and C84S were both predominantly dimer under the same conditions (Supplementary Figure S6A). Interestingly, H89A(site 3) and H90A(site 2) also showed defects in dimer formation under the same conditions, albeit to a lesser extent compared to H124A (Supplementary Figure S6C and D). These residues are in the same loop which physically connects site 2 and site 3. These data suggest that mutations in this loop may perturb the local conformation, and thereby lead to a less stable dimer.

Stepwise activation of BsZur–DNA interaction

Next, we sought to determine which of the various metal-bound states of BsZur is correlated with DNA-binding and therefore repression of gene expression. DNA binding of WT and BsZur mutants was determined using a fluorescence anisotropy (FA) assay with a *zur*-box DNA derived from the *yciA* promoter. As expected, WT BsZur bound DNA with high affinity under saturating Zn(II) conditions (Zur$_2$:Zn$_4$), but bound poorly in the absence of added Zn(II), resulting in a coupling free energy (ΔG_c) of -4.3 kcal/mol (Figure 4A, Table 2). We then took advantage of the fact that both site 2 mutant proteins (C84S and H90A) retained near wild-type affinity for the first Zn(II) binding event (K_{Zn1}) but had significantly decreased affinity for the second event (K_{Zn2}; Table 1). This enables population of a distinct asymmetric dimer (Zur$_2$:Zn$_3$). H90A, when fully loaded with Zn(II) (Zur$_2$:Zn$_4$), bound the DNA with similar affinity as WT (Figure 4B, Table 2). However, when NTA [$K_{Zn} = 8.7 \times 10^8\,M^{-1}$ at pH 8.0 (32)] was present to assure a Zur$_2$:Zn$_3$ form, H90A bound the DNA with an intermediate affinity, resulting in a partially activated state (Figure 4B). In this case, the energetic contribution of Zn(II) binding to DNA affinity (the coupling free energy) was about half of that of Zur$_2$:Zn$_4$ ($\Delta G_c = -2.0$ kcal/mol; Table 2). Thus, for the H90A mutant protein, there is a stepwise activation by the two Zn(II) ions binding to the BsZur dimer: the first interaction at the sensing site partially activates the protein (K_a ~$2.8 \times 10^6\,M^{-1}$) while the second binding event leads to even higher DNA binding affinity (K_a ~$8.2 \times 10^7\,M^{-1}$) (Figure 4D).

Surprisingly, when the same experiment was carried out using C84S BsZur, we noticed that it bound the DNA with relatively low affinity (comparable to the Zur$_2$:Zn$_3$ form of H90A) even in the presence of saturating Zn(II). The same experiment done in presence of NTA revealed no change in binding affinity (Figure 4C, Table 2). This suggests that the DNA binding of C84S only depends on the first Zn(II) binding (K_{Zn1}) to the sensing site in the dimer but not the second (K_{Zn2}). Since C84S still forms a stable dimer, we conclude that this moderate DNA binding affinity may be the reason why it only partially represses gene expression *in vivo*. These results led us to hypothesize that WT BsZur may also be activated to bind DNA by two sequential Zn(II) sensing events (simulated dotted curve, Figure 4A). Unfortunately, we were unable to make a homogeneous Zur$_2$:Zn$_3$ form of WT BsZur based on the measured K_{Zn1} and K_{Zn2}. Therefore, an alternative approach was applied as below.
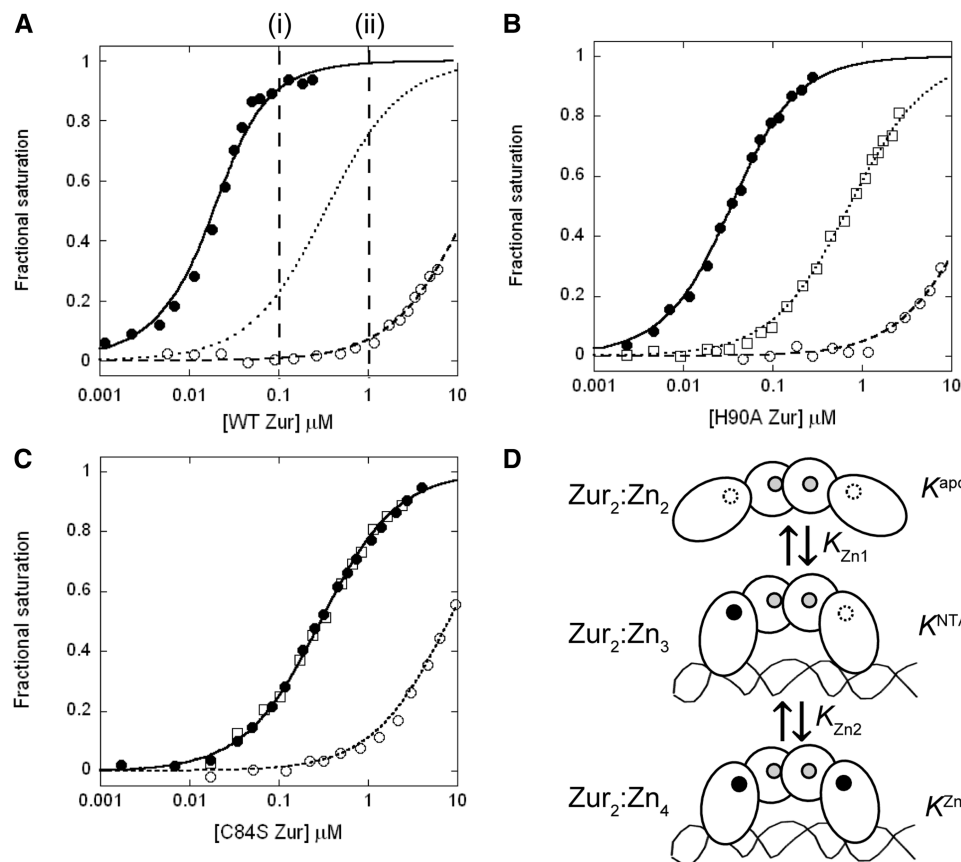
Figure 4. Binding of WT (**A**), H90A (**B**) and C84S (**C**) BsZur proteins to the *yciA zur*-box in the presence of saturating Zn(II) (filled circle, solid line), NTA (open square, dotted line) or EDTA (open circle, dashed line). All curves represent the best fit to a 1:1 non-dissociable:DNA binding model except for the dotted line in (A), which is a simulated curve based on the theoretical value calculated in Table 1. (i) and (ii) in (A) represent the two conditions under which Zn(II) activation assays were carried out for Figure 5 (see text). (**D**) The stepwise activation model of BsZur.

Table 2. DNA binding of BsZur to *zur*-box derived from *yciA* promoter

BsZur	K^{Zn} ($\times 10^7 M^{-1}$)	K^{NTA} ($\times 10^7 M^{-1}$)	K^{apo} ($\times 10^5 M^{-1}$)	$\Delta G_c^{NTA,a}$ (kcal/mol)	ΔG_c^a (kcal/mol)
WT	23 ($\pm$2)	0.61[b]	1.5 ($\pm$0.1)	−2.2[b]	−4.3 ($\pm$0.1)
C84S	0.70 ($\pm$0.01)	0.70 ($\pm$0.02)	2.5 ($\pm$0.1)	−2.0 ($\pm$0.0)	−2.0 ($\pm$0.0)
H90A	8.2 ($\pm$0.2)	0.28 ($\pm$0.01)	1.0 ($\pm$0.1)	−2.0 ($\pm$0.1)	−4.0 ($\pm$0.1)

[a]Calculated by $\Delta G_c^{NTA} = -RT\ln(K^{NTA}/K^{apo})$ and $\Delta G_c = -RT\ln(K^{Zn}/K^{apo})$ (34).
[b]Theoretical value calculated using $\Delta G_c^{NTA} = \Delta G_c/2$.

Sequential Zn(II) binding and sensing by WT BsZur

We reasoned that if DNA binding by WT BsZur was also activated stepwise by the sequential binding to two negatively cooperative sensing sites, the Zur_2:Zn_3 form would bind DNA with an intermediate affinity ($\Delta G_c = -2.2$ kcal/mol; $K^{NTA} = 6.1 \times 10^6 M^{-1}$) as noted by the simulated curve in Figure 4A. In this case, we calculated that nearly full activation of DNA binding would require the Zur_2:Zn_4 form at $0.10\,\mu M$ BsZur, while the Zur_2:Zn_3 form would suffice at $1.0\,\mu M$ Zur [vertical line (i) and (ii) in Figure 4A, respectively]. We therefore predict that demonstrably distinct free Zn(II) concentrations would be required to activate DNA binding at $0.10\,\mu M$ versus $1.0\,\mu M$ BsZur.

Measuring DNA binding affinity as a function of Zn(II) concentration using FA required the use of a Zn(II) chelator with a higher affinity than those used for the direct Zn(II)-binding studies above: just as Zn(II) binding increases BsZur affinity for DNA, cognate DNA increases the Zn(II) binding affinity. Therefore, a quantitative FA-based assay was designed in which the free Zn(II) concentration was 'buffered' by EDTA ($K_{Zn} = 1.8 \times 10^{14} M^{-1}$ at pH 8.0) (32). We anticipated that BsZur would bind Zn(II) in the presence of DNA with a femtomolar affinity comparable to that previously measured for EcZur and ScZur (18,21). Indeed, using a gel-based nuclease protection assay, we observed comparably high Zn(II) sensitivity for BsZur (at the *yciC* promoter) and EcZur (at the *znuC* promoter) (Supplementary Figure S7).

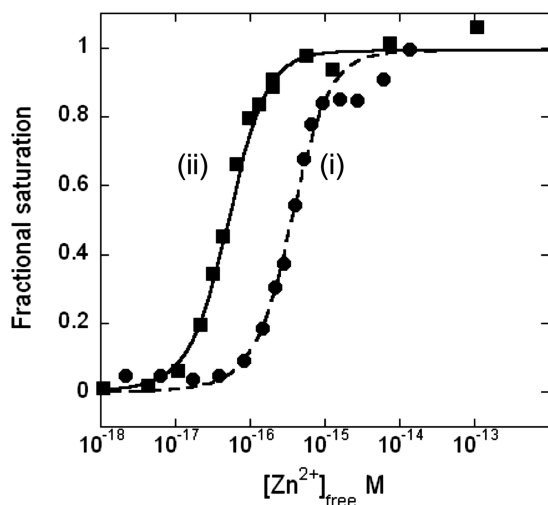When Zn(II) was titrated into a mixture of DNA, EDTA, with either 0.10 or $1.0\,\mu M$ BsZur, two distinct

Figure 5. DNA binding by WT BsZur is activated by femtomolar free Zn(II). Data fitting reveals K_{Zn} of (i) 2.4 ($\pm$0.1) $\times 10^{14}\,M^{-1}$ for 0.1 μM BsZur and (ii) 1.7 ($\pm$0.1) $\times 10^{15}$ for 1.0 μM BsZur.

activation curves resulted (Figure 5). Note that a 7-fold higher free Zn(II) concentration was required to fully activate DNA binding with only 0.10 μM Zur monomer. These data are best fit to two sequential Zn(II) sensing events to generate the active $Zur_2{:}Zn_4$ form with K_{Zn} of 1.7 ($\pm$0.1) $\times 10^{15}\,M^{-1}$ and 2.4 ($\pm$0.1) $\times 10^{14}\,M^{-1}$. This provides further support for the stepwise activation model for WT BsZur and indicates that BsZur senses Zn(II) with femtomolar affinity (Figures 4D and 5).

DISCUSSION

The presence of both metal binding sites 2 and 3 in many Fur family proteins (in addition to a structural Zn(II) site, when present) has confounded attempts to assign the location of metal sensing. Unlike HpFur and ScZur, where both site 2 and 3 were visualized to bind metal ions by crystallography and suggested to participate in metal sensing (14,18), we assign the metal sensing role in BsZur to site 2: site 3 does not bind metal ions with a physiologically relevant affinity, although residues in this region do contribute to dimer stability. This finding shares some similarity with BsPerR, where the corresponding site 3 residues do not bind metal and are proposed to form a hydrogen-bonding network which affects metal selectivity at site 2 (13). Such interactions may be present in BsZur as well to modulate dimer stability. In fact, in the crystal structure of MtZur, although a Zn(II) atom was bound at the corresponding site 3, the protein appeared to be in an open conformation not optimal for DNA binding (16). It is thus possible that hydrogen bonding interactions instead of metal binding in this hinge region may facilitate the closed conformation for high affinity DNA interaction.

Our results suggest that the roles of sites 2 and 3 may vary in different Fur family proteins. In HpFur and ScZur both site 2 and site 3 were occupied by Zn(II) ions and both sites may be involved in metal sensing (14,18). Although Co(II) binding studies with HpFur revealed distinct spectral features consistent with complexes at sites 2 and 3, the binding stoichiometry appeared to be only one per monomer (14,18). In fact, among all the Fur family proteins in which both site 2 and 3 were visualized to bind metal ions in the crystal structures, functional occupancy of both sites has never been demonstrated. Our data show clearly a maximal stoichiometry of 2 Zn(II) per BsZur monomer (including structural site 1), thereby indicating that only one additional site (assigned as site 2) is required for metal sensing. Our results also contrast with recent findings with ScZur which suggest a graded response for different *zur*-regulated genes based on Zn(II) availability (18). In this case, ScZur was found to have subtly different DNA binding affinities for different operator DNAs. Using promoter–*lacZ* fusions, we tested the Zn(II) concentrations required to repress each Zur regulon promoter. However, no differential response was noted *in vivo*. Further *in vitro* measurement of the DNA binding affinities using FA revealed that WT BsZur binds to the *ytiA* and *yciA* operators with nearly identical affinities.

In the stepwise activation model proposed here, two distinct DNA binding conformations are achieved by the sequential and negatively cooperative binding of Zn(II) to the BsZur dimer (Figure 4D). This predicts that BsZur may respond to a wider range of intracellular Zn(II) concentrations to gradually repress genes. In fact, negatively cooperative metal binding has been documented in many metalloregulators, and in the extreme case of MerR leads to full activation with a stoichiometry of 1 Hg(II) per dimer (33). One possible advantage of two, negatively cooperative binding events is that, rather than a two-state 'on' and 'off' switch, such proteins may sense a broader range of intracellular metal ion concentrations.

BsZur, like other metalloregulatory proteins, dictates the 'set-point' around which intracellular (free) Zn(II) concentrations fluctuate. Our results highlight the finding that Zur proteins maintain intracellular free Zn(II) levels in the femtomolar range. In addition, our results reveal that the intracellular concentration of the regulator (BsZur) can also be an important variable in dictating this 'set-point' as inferred by an *in vitro* Zn(II) activation assay (Figure 5). Thus, variations in metalloregulator concentrations can also affect metal-ion homeostasis. In fact, many metalloregulators are auto-regulated and the resulting changes in protein level could therefore lead to a 'reset' of the set-point for intracellular concentrations of the cognate metal ion. For instance, such 'reset' may allow the cell to decrease the intracellular Zn(II) level by 1–2 orders of magnitude in the case of *S. aureus* CzrA, which is auto-regulated and also displays negatively cooperative Zn(II) binding (31). Clearly, a complete understanding of metalloregulatory circuits will require consideration of the proteins affinities for all relevant ligands as well as their energetic coupling.

REFERENCES

1. Lee,J.W. and Helmann,J.D. (2007) Functional specialization within the Fur family of metalloregulators. *BioMetals*, **20**, 485–499.
2. Ma,Z., Jacobsen,F.E. and Giedroc,D.P. (2009) Coordination chemistry of bacterial metal transport and sensing. *Chem. Rev.*, **109**, 4644–4681.
3. Hantke,K. (1981) Regulation of ferric iron transport in *Escherichia coli* K12: isolation of a constitutive mutant. *Mol. Gen. Genet.*, **182**, 288–292.
4. Gaballa,A., Antelmann,H., Aguilar,C., Khakh,S.K., Song,K.-B., Smaldone,G.T. and Helmann,J.D. (2008) The *Bacillus subtilis* iron-sparing response is mediated by a Fur-regulated small RNA and three small, basic proteins. *Proc. Natl Acad. Sci. USA*, **105**, 11927–11932.
5. Ollinger,J., Song,K.-B., Antelmann,H., Hecker,M. and Helmann,J.D. (2006) Role of the Fur regulon in iron transport in *Bacillus subtilis*. *J. Bacteriol.*, **188**, 3664–3673.
6. Gaballa,A., Wang,T., Ye,R.W. and Helmann,J.D. (2002) Functional analysis of the *Bacillus subtilis* Zur regulon. *J. Bacteriol.*, **184**, 6508–6514.
7. Gabriel,S.E. and Helmann,J.D. (2009) Contributions of Zur-controlled ribosomal proteins to growth under zinc starvation conditions. *J. Bacteriol.*, **191**, 6116–6122.
8. Lee,J.W. and Helmann,J.D. (2006) The PerR transcription factor senses H_2O_2 by metal-catalysed histidine oxidation. *Nature*, **440**, 363–367.
9. Lee,J.W. and Helmann,J.D. (2006) Biochemical characterization of the structural Zn^{2+} site in the Bacillus subtilis peroxide sensor PerR. *J. Biol. Chem.*, **281**, 23567–23578.
10. Bsat,N. and Helmann,J.D. (1999) Interaction of *Bacillus subtilis* Fur (ferric uptake repressor) with the dhb operator in vitro and in vivo. *J. Bacteriol.*, **181**, 4299–4307.
11. Jacquamet,L., Traoré,D., Ferrer,J.-L., Proux,O., Hazemann,J.-L., Nazarenko,E.E., Ghazouni,A., Caux-Thang,C., Duarte,V. and Latour,J.-M. (2009) Structural characetrization of the active form of PerR: insights into the metal-induced activation of PerR and Fur proteins for DNA binding. *Mol. Microbiol.*, **72**, 20–31.
12. Traore,D.A.K., Ghazouani,A.E., Jacquamet,L., Borel,F., Ferrer,J.-L., Lascoux,D., Ravanat,J.-L., Jaquinod,M., Blondin,G., Caux-Thang,C. *et al.* (2009) Structural and functional characterization of 2-oxo-histidine in oxidized PerR protein. *Nat. Chem. Biol.*, **5**, 53–59.
13. Ma,Z., Lee,J.-W. and Helmann,J.D. (2011) Identification of altered function alleles that affect *Bacillus subtilis* PerR metal ion selectivity. *Nucleic Acids Res.*, **39**, 5036–5044.
14. Dian,C., Vitale,S., Leonard,G.A., Bahlawane,C., Fauquant,C., Leduc,D., Muller,C., de Reuse,H., Michaud-Soret,I. and Terradot,L. (2011) The structure of the *Helicobacter pylori* ferric uptake regulator Fur reveals three functional metal binding sites. *Mol. Microbiol.*, **79**, 1260–1275.
15. Pohl,E., Haller,J.C., Mijovilovich,A., Meyer-Klaucke,W., Garman,E. and Vasil,M.L. (2003) Architecture of a protein central to iron homeostasis: crystal structure and spectroscopic analysis of the ferric uptake regulator. *Mol. Microbiol.*, **47**, 903–915.
16. Lucarelli,D., Russo,S., Garman,E., Milano,A., Meyer-Klaucke,W. and Pohl,E. (2007) Crystal structure and function of the zinc uptake regulator FurB from *Mycobacterium tuberculosis*. *J. Biol. Chem.*, **282**, 9914–9922.
17. Sheikh,M.A. and Taylor,G.L. (2009) Crystal structure of the *Vibrio cholerae* ferric uptake regulator (Fur) reveals insights into metal co-ordination. *Mol. Microbiol.*, **72**, 1208–1220.
18. Shin,J.-H., Jung,H.J., An,Y.J., Cho,Y.-B., Cha,S.-S. and Roe,J.-H. (2011) Graded expression of zinc-responsive genes through two regulatory zinc-binding sites in Zur. *Proc. Natl Acad. Sci. USA*, **108**, 5045–5050.
19. Outten,C.E., Olson,K.E., Cao,H. and O'Halloran,T.V. (1999) The ferric uptake regulation (Fur) repressor is a zinc metalloprotein. *Biochemistry*, **38**, 6559–6569.
20. Outten,C.E., Tobin,D.A., Penner-Hahn,J.E. and O'Halloran,T.V. (2001) Characterization of the metal receptor sites in *Escherichia coli* Zur, an ultrasensitive zinc(II) metalloregulatory protein. *Biochemistry*, **40**, 10417–10423.
21. Outten,C.E. and O'Halloran,T.V. (2001) Femtomolar sensitivity of metalloregulatory proteins controlling zinc homeostasis. *Science*, **292**, 2488–2492.
22. Mills,S.A. and Marletta,M.A. (2005) Metal binding characteristics and role of iron oxidation in the ferric uptake regulator from *Escherichia coli*. *Biochemistry*, **44**, 13553–13559.
23. Gaballa,A. and Helmann,J.D. (1998) Identification of a zinc-specific metalloregulatory protein, Zur, controlling zinc transport operons in *Bacillus subtilis*. *J. Bacteriol.*, **180**, 5815–5821.
24. Slack,F.J., Mueller,J.P. and Sonenshein,A.L. (1993) Mutations that relieve nutritional repression of the Bacillus subtilis dipeptide permease operon. *J. Bacteriol.*, **175**, 4605–4614.
25. Miller,J.H. (1972) *Experrmiments in Molecular Genetics*. Cold Spring Harbor Laboratory, Cold Spring Harbor, NY.
26. Gabriel,S.E., Miyagi,F., Gaballa,A. and Helmann,J.D. (2008) Regulation of the *Bacillus subtilis* yciC gene and insights into the DNA-binding specificity of the zinc-sensing metalloregulator Zur. *J. Bacteriol.*, **190**, 3482–3488.
27. Kuzmic,P. (1996) Program DYNAFIT for the analysis of enzyme kinetic data: application to HIV proteinase. *Anal. Biochem.*, **237**, 260–273.
28. Gee,K.R., Zhou,Z.-L., Qian,W.-J. and Kennedy,R. (2002) Detection and imaging of zinc secretion from pancreatic β-cells using a new fluorescent zinc indicator. *J. Am. Chem. Soc.*, **124**, 776–778.
29. Jefferson,J.R., Hunt,J.B. and Ginsburg,A. (1990) Characterization of indo-1 and quin-2 as spectroscopic probes for Zn^{2+}-protein interactions. *Anal. Biochem.*, **187**, 328–336.
30. Corwin,D.T., Fikar,R. and Koch,S.A. (1987) Four- and five-coordinate cobalt(II) thiolate complexes: models for the catalytic site of alcohol dehydrogenase. *Inorg. Chem.*, **26**, 3079–3080.
31. Pennella,M.A., Arunkumar,A.I. and Giedroc,D.P. (2006) Individual metal ligands play distinct functional roles in the zinc sensor *Staphylococcus aureus* CzrA. *J. Mol. Biol.*, **356**, 1124–1136.
32. Martell,A.E. and Smith,R.M. (1979-1989) *Critical Stability Constants*. Plenum Press, New York.
33. Helmann,J., Ballard,B. and Walsh,C. (1990) The MerR metalloregulatory protein binds mercuric ion as a tricoordinate, metal-bridged dimer. *Science*, **247**, 946–948.
34. Reyes-Caballero,H., Campanello,G.C. and Giedroc,D.P. (2011) Metalloregulatory proteins: metal selectivity and allosteric switching. *Biophys. Chem.*, **156**, 103–114.